

Supporting Information

Spatially resolved multimodal vibrational spectroscopy under high pressures

Sabine N. Neal, Dario Stacchiola, and Samuel A. Tenney

Methods

O-PTIR and Raman Spectroscopy

Spectra and images were collected on a mIRage infrared and Raman microscope (Photothermal Spectroscopy Corp.). Sample collection was completed via a pulsed, tunable quantum cascade laser (QCL) focused through a 40X, .78 NA objective onto the sample surface. Infrared background spectra were collected on a low emissivity standard, with the QCL set to 100% power, probe beam from 11-22% power, a pulse rate of 100 kHz, and a pulse width of 500 ns over the frequency range of 758-1806 cm^{-1} . IR scans were taken at 6.6 cm^{-1} spectral resolution. Sample spectra were collected on an organic material, with the QCL set to 22% and the probe beam to 11% power. Sample spectra were averaged over 5 sweeps and were taken at 6.6 cm^{-1} spectral resolution. All sample spectra were normalized to the collected background spectrum. Raman scattering was detected by a Horiba IHR320 module using the 600 groove/mm grating and collected using a 1 s integration with 30 scans co-averaged over the frequency range of 50 - 4000 cm^{-1} . The hyperspectral images were collected over a 20 μm x 20 μm area, a resolution of 41 x 41 points, and a spacing of 0.5 μm x 0.5 μm .

Pressure Studies

High quality crystalline MoO_3 was grown via chemical vapor transport and was purchased from 2D Semiconductors. Blended samples composed of HMX, CL-20, and a fluorinated organic binder were received from Picatinny Arsenal (Wharton, NJ). Individual samples were loaded into the diamond anvil cell along with an annealed ruby ball (Fig. 3(a)). Spectroscopic data was collected employing an in-house modified diamond anvil cell (Almax easyLab) equipped with a type II diamond by direct fluorescence measurements of the *R1* ruby line.¹ The diamond cutlets were 0.80mm. The gaskets were 304L stainless steel and the hole diameter was 320 μm . Infrared measurements were collected over the frequency range of 758-1806 cm^{-1} with the infrared-QCL set to 22% and the probe beam to 11%. All sample spectra were normalized to the collected background spectrum. Raman scattering measurements were collected simultaneously using the 600 groove/mm grating with 1 s integration and 30 scans co-averaged across the 50-4000 cm^{-1} frequency range. Spectra were collected from 0 to 13 GPa.

Experimental Pressure Studies

Preliminary pressure studies have been completed using traditional diamond anvil cell techniques. Figure S1 depicts the resulting Raman spectra of crystalline MoO₃ as a function of pressure. There is a noticeable blueshift in frequency in all modes as pressure is increased from 0 to 2.23 GPa, and upon release in pressure down to 1.48 GPa the features slightly redshift. This blueshift is evidenced in Fig. S1 (right panel), showing peak position as a function of pressure. This is a common trend in pressures studies, where the blueshift in this frequency range is likely indicative of an increase in bond length, which as been confirmed in previous pressure work on MoO₃, revealing higher order structural transitions occurring at 12 GPa and 25 GPa.²

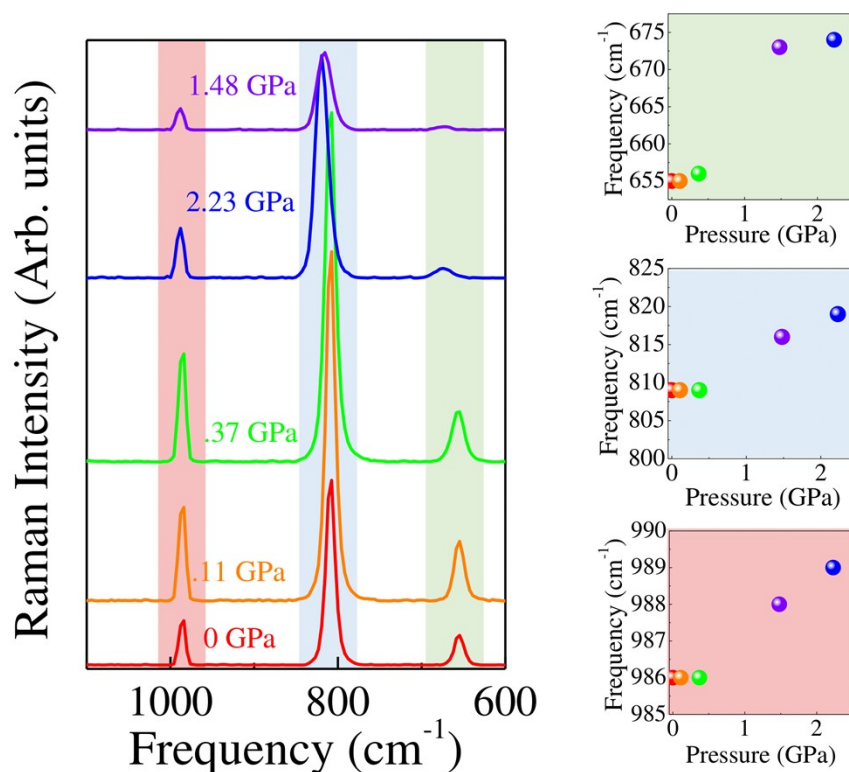


Fig. S1 Displays the Raman spectra of MoO₃ as a function of pressure. The peak positions of the highlighted features are shown as well, with the colors of the points corresponding to the specific pressures.

Figure S2 shows the Raman and O-PTIR spectra of a common high energy material, CL-20, as a function of pressure. Figure S2(a) shows the Raman spectra across the full frequency window for this system, with close-ups of spectral features in Panels (b) and (c). Again, as was seen in the previous Raman studies most features blueshift as pressure is increased, with a red shift upon

release. This is especially noticeable in the features near 812 cm^{-1} [Panel(b)] and the mode centered around 1325 cm^{-1} [Panel (c)], however some features seen at ambient pressure in Panel (b) deviate from this trend. Taking a closer look, there does appear to be a loss of a mode around 250 cm^{-1} above $.85\text{ GPa}$, along with the low frequency doublet merging into one broad peak just near 5.63 GPa . These are likely due to a structural phase transition from $\epsilon \rightarrow \gamma$ CL-20 phase. Similar results have been reported in literature.³

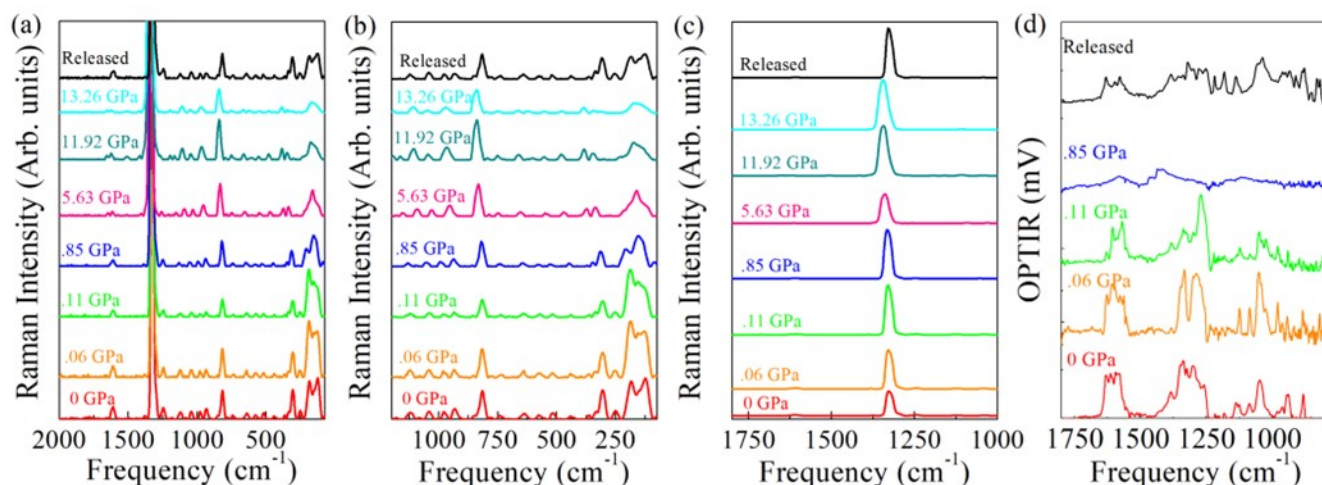


Fig. S2 Panel(a) shows a complete look at the Raman spectra under pressure of a high energy system, CL-20, with Panels (b and c) depicting close-up views of specific areas of interest. Panel(d) shows the correlating O-PTIR spectra of CL-20 as a function of pressure.

Taking a closer look at the corresponding infrared spectra (Fig. S2(d)), the slight blueshift is again present overall as pressure is increased with the presence of the previously mentioned structural change also seen here ($\sim 1300\text{ cm}^{-1}$) beginning as low as $.06\text{ GPa}$ and continuing until $.86\text{ GPa}$. However, notice there is a complete lack of signal near $.86$, due to the inability of the material to expand at high pressure. When pressure is released slightly in the cell, the features reappear. From 0 to $.06\text{ GPa}$ there is no noticeable change in the Raman, however the IR is clearly showing a chemical or structural change is already occurring, again emphasizing the need for multimodal measurements under the same exact conditions and from the same region of the sample.

Table S1: Displays both the O-PTIR and Raman vibrational mode assignments for the CL-20 system. These assignments were completed using prior literature.³

O-PTIR	Raman	Assignment
-	125	NO ₂ deformation
-	185, 252, 308, 36, 365	C-N-C band + torsion/ring motion
-	440, 521, 575, 643	Ring motion and scissoring NO ₂
-	742	NO ₂ deformation
798, 819, 834, 858, 879, 910, 937, 959, 979, 1023, 1050, 1079	786, 816, 850, 879, 909, 933, 974, 979, 1002, 1036	Symmetric ring stretch
1105, 1124, 1153	1042, 1070, 1081	N-N stretch
-	1122	C-H stretch
-	1159	C-N-N asymmetric stretch
1180	1173, 1179, 1188	Ring stretch/C-N-C stretch
-	1196, 1204	C-H bending

1222	1211, 1246	Ring stretch
1239, 1259, 1269, 1291, 1332	1262	NO ₂ symmetric stretch
1347, 1383	1374, 1381, 1465, 1476	CH ₂ mode deformations
1562	1492, 1496, 1505, 1564, 1578	NO ₂ asymmetric stretch
-	1610	CN stretch/NH bend
-	3040	CH ₂ stretch

1. H. K. Mao, P. M. Bell, J. W. Shaner and D. J. Steinberg, *Journal of Applied Physics*, 1978, **49**, 3276–3283.
2. D. Liu, W. W. Lei, J. Hao, D. D. Liu, B. B. Liu, X. Wang, X. H. Chen, Q. L. Cui, G. T. Zou, J. Liu and S. Jiang, *Journal of Applied Physics*, 2009, **105**, 1–8.
3. J. C. Gump, *Journal of Physics: Conference Series*, 2014, **500**, 052014.